J. Fluid Mech. (1977), *vol.* 79, *part* 3, *pp.* 595–607
Printed in Great Britain

Intermittency in a thermal mixing layer

By J. F. KEFFER, G. J. OLSEN AND J. G. KAWALL
Department of Mechanical Engineering, University of Toronto, Canada M5S 1A4

(Received 27 November 1974 and in revised form 22 October 1975)

An investigation of the existence of purely thermal intermittency has been undertaken for the flow produced by a step change in temperature in a decaying homogeneous turbulent field. The results show that a thermal interface can be defined and that it is a random function of space and time, having gross characteristics similar to the turbulent interface in a free shear flow. A technique for identifying the hot and cold regions of the fluid in a systematic way was developed and this permitted conditional averages of the mean and fluctuating temperature to be formed.

1. Introduction

The mechanism by which a scalar contaminant spreads in a turbulent flow is an interesting and important question; it has, as a result, been the subject of considerable research. One very simple realization of the problem is to introduce a step change in the concentration level of the contaminant within a homogeneous turbulent field and examine the characteristics of the subsequent spread and diffusion in the streamwise direction. We have effected this realization using heat as the contaminant, which for small temperature differences can be considered as a passive scalar. Specifically, the requirement is that the ratio of buoyancy to inertial and viscous effects be arbitrarily small.

The present investigation is a general extension of the early work of Mills & Corrsin (1959), Gibson & Schwarz (1963) and others who examined the decay of contaminant fluctuations in homogeneous turbulent fields. The problem was extended by Wiskind (1962), who introduced a constant linear mean temperature gradient, thus establishing a source or generation of the contaminant. A further stage of complexity is the inhomogeneous situation which occurs in a mixing layer. Watt (1967), Watt & Baines (1973) and more recently Fiedler (1974) examined both the velocity and the temperature mixing layer. In our case, we consider the pure thermal mixing layer only and direct attention to the interfacial characteristics of the motion since these determine the way in which the heat propagates into the colder region of the flow.

An analogous situation is the spread of a turbulent front at the edge of a free shear flow. Corrsin (1943) was the first to recognize that the interface which separates the turbulent and non-turbulent fluid is sharp. Furthermore it can be considered a random function of space and time, so that a fixed probe placed in this region will yield a signal which is intermittently turbulent. Much work has

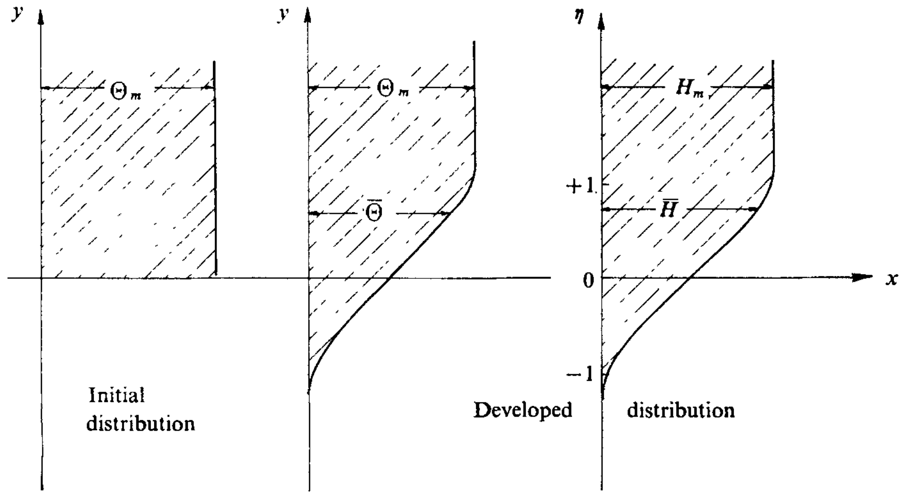

FIGURE 1. Definition sketch of developing flow.
$\bar{H} = \bar{\Theta}/\Theta_m$, $H_m = 1$, $\eta = (y - y_{\bar{H}=0\cdot5})/l_\theta$, $l_\theta = y_{\bar{H}=0\cdot9} - y_{\bar{H}=0\cdot1}$.

been carried out in establishing the characteristics of the intermittency for various shear flows. More recently, the use of heat as a tracer has proved to be a valuable adjunct in identifying the interface (LaRue 1974; Antonia & Bilger 1974; Davies, Keffer & Baines 1975; among others). The implication is that the turbulent fluid is marked uniquely by the temperature, independent molecular conduction across the interface being negligible.

By analogy it might be expected that an equivalent, purely thermal intermittency would be observed in the present flow. The transfer of heat must be accomplished by the convective action of the turbulent eddies, but in this homogeneous turbulent flow, at any given point only a fraction of the eddies will be tagged by the temperature. In the results which follow we show that such thermal intermittency can be identified. Furthermore it is possible to define zone averages for the hot and cold fluid using what can be considered now as conventional conditional sampling techniques.

2. Experimental approach

The experiments were carried out in a small open-circuit wind tunnel with test section $0{\cdot}23 \times 0{\cdot}46$ m and $1{\cdot}25$ m long. In the settling chamber prior to the test section a heating grid was installed. This consisted of a rack of cylinders, $9{\cdot}5$ mm in diameter, mounted horizontally, with centre-to-centre spacing of $M = 25$ mm. Each cylinder was electrically heated and controlled individually by a variac. For the present experiment the upper half of the grid was heated uniformly and the profile allowed to develop as shown schematically in figure 1. The temperature Θ was defined as the difference between the flow temperature and the ambient temperature, and the dimensionless quantity H as the ratio Θ/Θ_m, where Θ_m is the maximum mean temperature difference.

Temperature signals were obtained with a DISA 55M20 constant-current bridge operating a platinum-plated resistance thermometer, or 'cold wire',

η	$\overline{\Theta}$ (°K)	$(\overline{\theta^2})^{\frac{1}{2}}$ (°K)	L_θ (mm)	λ_θ (mm)	χ (°K^2 s^{-1})
1·0	4·30	0·167	51·0	5·8	0·228
0	2·13	0·640	22·0	5·5	3·76

TABLE 1. Thermal characteristics, $x/M = 41{\cdot}0$. The dissipation χ was estimated from the isotropic relation $\chi = 12\alpha(\overline{\theta^2})^{\frac{1}{2}}/\lambda_\theta^2$, where α is the thermal diffusivity. L_θ and λ_θ were obtained from the spectra of the temperature fluctuation intensity.

Mean velocity	$U_0 = 9{\cdot}0\ \mathrm{m\,s^{-1}}$
Longitudinal turbulent velocity	$(\overline{u^2})^{\frac{1}{2}} = 0{\cdot}28\ \mathrm{m\,s^{-1}}$
Turbulent intensity	$(\overline{u^2})^{\frac{1}{2}}/U_0 = 0{\cdot}0315$
Macroscale	$L_u = 18\ \mathrm{mm}$
Microscale	$\lambda_u = 4{\cdot}3\ \mathrm{mm}$
Kolmogorov scale	$l_s = (\nu^3/\epsilon)^{\frac{1}{4}} = 0{\cdot}24\ \mathrm{mm}$
Dissipation rate	$\epsilon = 1{\cdot}14\ \mathrm{m^2\,s^{-3}}$

TABLE 2. Velocity characteristics, $x/M = 41{\cdot}0$. The dissipation rate was obtained from the isotropic relation $\epsilon = 15\nu(\overline{u^2})^{\frac{1}{2}}/\lambda_u^2$. Micro- and macroscales were obtained from the spectra of the turbulent intensity.

$1\,\mu$m in diameter and 0·4 mm long. The wire heating current was low enough that parasitic influence of the velocity fluctuations was negligible. In addition the convection velocity was high enough and the maximum temperature difference low enough so that thermal lag from the prongs of the probe was not a factor. The upper frequency limit of the system was 3 kHz at 10 m s^{-1}. The signals were low-pass filtered at 2 kHz, which was high enough to retain the significant energy content of the thermal signal.

Using the system described by Hedley & Keffer (1974*a*), the output from the anemometer was sampled digitally at 5000 points/s to prevent aliasing. These data were stored on magnetic tape and processed on the University of Toronto Computer Center IBM 370 Model 165, which has 3 megabytes of core. Twenty seconds of data were recorded for each point, giving 100 000 samples. These were sufficient to determine stable mean and r.m.s. intensity levels for the signal.

Alexopoulos & Keffer (1971) showed that, for the usual operating conditions in this tunnel, density differences are negligible. For example, consider the dimensionless group

$$g\beta l\Theta_m/U_0^2,$$

which can be considered as the ratio of the Grashof number to the square of the Reynolds number. For the typical values velocity $U_0 = 6{\cdot}1$ m s^{-1}, tunnel height $l = 0{\cdot}46$ m, maximum mean temperature difference $\Theta_m = 5$ °K and coefficient of thermal expansion $\beta = 1/T = 293$ °K^{-1}, the above expression is about 0·002, which is small enough for the temperature to be considered a truly passive contaminant.

Thermal and velocity characteristics are given in tables 1 and 2 respectively, for the streamwise station $x/M = 41$.

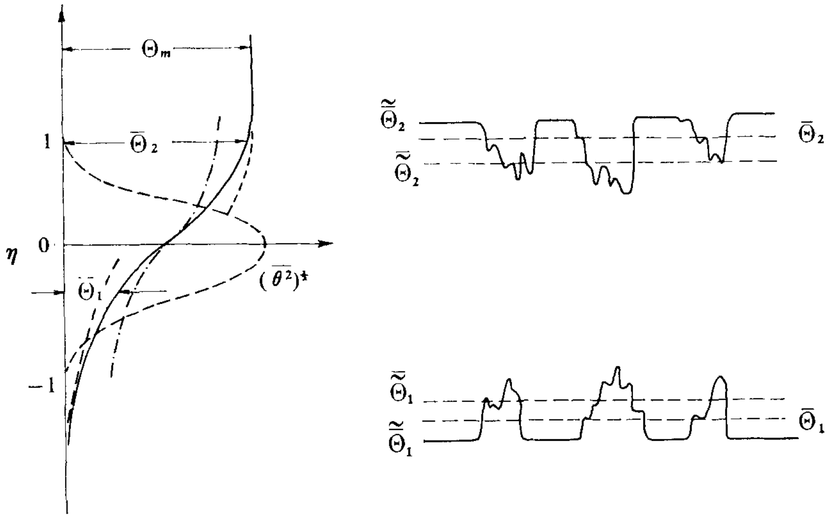

FIGURE 2. Definition sketch of zone-averaged quantities.

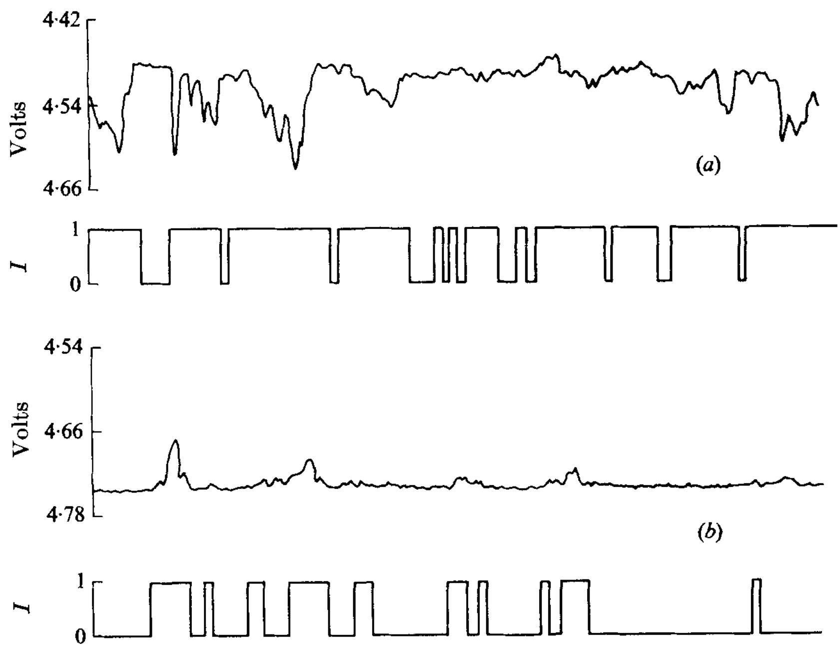

FIGURE 3. Representative signal traces with indicator function; $x/M = 41$. (*a*) $\eta = 0{\cdot}44$, (*b*) $\eta = 0{\cdot}73$.

3. Characteristics of the temperature signal

The qualitative behaviour of the intermittent thermal signals is illustrated schematically in figure 2. Warm fluid is convected by turbulent eddies into the colder region of the flow, resulting in the 'burst' pattern suggested by trace 1. A similar situation occurs in the upper, hot region except that there the 'bursts' are not as hot as the background flow. In principle one would expect the thermal characteristics to exhibit this symmetry. The contaminant, if truly passive, cannot affect the random convective motion of the turbulent field and thus all turbulent eddies have equal probability of moving into the hot or cold region of the mixing layer, regardless of their temperature level.

Justification for this assumption is given by typical signal outputs for the two regions, shown in figure 3. An intermittent nature of the flow truly exists and the problem reduces to a search for a suitable method of identifying the hot and cold zones.

4. Generation of the indicator function

The technique for distinguishing between two fluid states such as the turbulent and non-turbulent flow at the outer edges of, say, a turbulent boundary layer is subject to a certain arbitrariness (Hedley & Keffer 1974*b*). In the present case, however, it might seem that the problem is more straightforward. In principle, the temperature signal itself, rather than some complicated, sensitized variable of the thermal field, should be able to provide a direct means for identifying the hot or cold zones. In fact, after some trial it was concluded that rather more sensitive discrimination would be obtained by using the square of the derivative of the local temperature $(\partial\Theta/\partial t)^2$. The advantage of using this signal for detection is that burst activity is emphasized, while background noise fluctuations, generally of low amplitude, are attenuated.

Like any quantity associated with the turbulent field, the detector signal is a random function. A finite probability exists, therefore, that it can be zero while still within a positive detecting mode. Such signal drop-out can be eliminated by a number of methods each of which involves some subjectivity. In the present case, following the technique of Hedley & Keffer (1974*b*), we used a smoothing time with a length based on the Taylor microscale of the thermal fluctuation intensity,

$$\tau_\theta = \langle\overline{\theta^2}/\overline{(\partial\Theta/\partial t)^2}\rangle^{\frac{1}{2}}.$$

An alternative technique, suggested by Bradshaw & Murlis (1973), where the derivative of the detector function is used in an either/or mode as a back-up, was considered. We found, however, that for these circumstances a smoothing of the back-up function was then required to eliminate signal drop-out of the derivative. The situation is analogous to the closure problem in theoretical approaches to turbulence. In principle we should probably require an infinite number of higher-derivative functions for successive back-up. In actual fact, three functions would perhaps suffice but for the present circumstance we felt that smoothing over four data points ($0{\cdot}8\times10^{-3}$ s or approximately τ_θ), initially with a single function, was a more direct and certainly simpler approach. The criterion function S_1, which is defined as the smoothed detector function, is, in digital form,

$$S_1(i\Delta t) = \frac{1}{T_s}\sum_{j=i-\frac{1}{2}N_s}^{i+\frac{1}{2}N_s}\left(\frac{\Delta\Theta}{\Delta t}\right)_j^2,$$

where Δt is the resolution of the digital signal, T_s is the smoothing time and $N_s = T_s/\Delta t$.

The final stage requires the application of a threshold level. To choose this setting, we appeal to the physical nature of the flow. The plane of symmetry for the thermal field is the lateral position where $\overline{\Theta}/\Theta_m = 0{\cdot}5$. At this point, the thermal fluctuation intensity $(\overline{\theta^2})^{\frac{1}{2}}$ is a maximum (Watt 1967) and we may consider the thermal fluctuation field to be locally homogeneous. The intermittency factor γ is therefore unity by definition. We consider first the lower or cold region of the mixing layer. The threshold level C_1 required to generate $\gamma = 1$ at this point was determined from the 99 % value on the probability density function of $(\partial\Theta/\partial t)^2$, plotted with respect to C_1. Similarly, at a y position in the fully cold zone, where inspection of the temperature traces revealed no hot bursts, the threshold level was taken as the 99 % point of the corresponding probability density function for the cold fluid. This determined the value of C_1 required to produce $\gamma = 0$. The intersection of the probability density functions for these two cases was assumed to define the threshold level for $\gamma = 0{\cdot}5$. This threshold level was then applied to the complete set of data and a pseudo γ distribution constructed. The half-intermittency position could thus be identified. A smooth curve was then fitted through these three points to generate C_1 as a function of y, and the values given by this curve were used in the processing of all subsequent results. The above technique was used for the upper region of the flow, the hot zone, as well.

In the lower portion of the mixing layer it was found to be of some advantage to define a second criterion function S_2. The temperature signal Θ was used, with the threshold level set at three standard deviations of the background signal above its local mean. This background signal was extracted from the Θ signal by means of the first technique. The relatively high background 'noise', i.e. residual thermal fluctuations from the hot grid, in the upper zone precluded the application of the second technique in that region, however.

The procedures described above thus yielded the indicator functions:

$$I(y,t) = \begin{cases} 1 & \text{if} \quad S_1(y,t) > C_1(y) \quad \text{or} \quad S_2(y,t) > C_2(y) \\ 0 & \text{if} \quad S_1(y,t) \leqslant C_1(y) \end{cases}$$

for the lower region and

$$I'(y,t) = \begin{cases} 1 & \text{if} \quad S'_1(y,t) > C'_1(y) \\ 0 & \text{if} \quad S'_1(y,t) \leqslant C'_1(y) \end{cases}$$

for the upper region.

5. Properties of the flow

The intermittency factor γ was evaluated directly from

$$\gamma = \frac{1}{N\Delta t}\sum_{i=1}^{N} I(y,t_i)\,\Delta t, \tag{5.1}$$

where $t_i = i\Delta t$ and N is the number of discrete values of $I(y,t_i)$ in a time period T. The conventional and zone-averaged mean quantities are then

$$\overline{\Theta} = \frac{1}{N}\sum_{i=1}^{N} \Theta(t_i), \tag{5.2}$$

$$\bar{\bar{\Theta}} = \frac{1}{\gamma N} \sum_{i=1}^{N} \Theta(t_i)\, I(t_i), \tag{5.3}$$

$$\tilde{\bar{\Theta}} = \frac{1}{(1-\gamma)N} \sum_{i=1}^{N} \Theta(t_i)\,(1 - I(t_i)). \tag{5.4}$$

Equation (5.3) refers either to warm bursts in cold fluid (lower portion of mixing layer) or to warm bursts in hot fluid (upper portion). A similar distinction is made for (5.4) (refer to figure 2). Within each region, the above quantities will be related by

$$\bar{\Theta} = \gamma\bar{\bar{\Theta}} + (1-\gamma)\,\tilde{\bar{\Theta}}. \tag{5.5}$$

The corresponding fluctuation intensities are defined by

$$\overline{\theta^2} = \langle \Theta - \bar{\Theta} \rangle^2 \quad \text{averaged over entire signal,}$$

$$\overline{\tilde{\theta}^2} = \langle \Theta - \bar{\bar{\Theta}} \rangle^2 \quad \text{averaged over bursts only,}$$

$$\overline{\tilde{\tilde{\theta}}^2} = \langle \Theta - \tilde{\bar{\Theta}} \rangle^2 \quad \text{averaged over non-bursts only.}$$

The fluctuation intensities within each region will be related by

$$\overline{\theta^2} = \gamma\overline{\tilde{\theta}^2} + (1-\gamma)\,\overline{\tilde{\tilde{\theta}}^2} + \gamma(1-\gamma)\,(\bar{\bar{\Theta}} - \tilde{\bar{\Theta}})^2. \tag{5.6}$$

We note that, since $\bar{\bar{\Theta}}$ must always be quite different from $\tilde{\bar{\Theta}}$, the last term in (5.6) is always significant, unlike the corresponding term in the analogous equation for velocity fluctuations. It may be remarked that the accuracy with which (5.5) and (5.6) are satisfied by the various quantities depends only on the numerical technique used to evaluate these quantities. The technique used here produced essentially 100% accuracy.

The average durations of the hot and cold zones are defined as

$$\langle T \rangle_H = \frac{1}{M} \sum_{j=1}^{M} T_{Hj}, \quad \langle T \rangle_C = \frac{1}{M} \sum_{j=1}^{M} T_{Cj},$$

where M is the number of hot (or cold) zones which occur at a given point during a time T, T_{Hj} is the duration of the jth hot zone and T_{Cj} the duration of the jth cold zone, at the given point. With Taylor's hypothesis, these average zone times can be converted into average zone widths:

$$\langle L \rangle_H = U_0 \langle T \rangle_H, \quad \langle L \rangle_C = U_0 \langle T \rangle_C,$$

where U_0 is the velocity of the convecting flow.

The burst rate, which is the average number of hot (or cold) zones which occur at a given point per unit time, is given by

$$\hat{f} = M/T.$$

6. Results and discussion

Three streamwise situations were examined in detail: $x/M = 32$, 41 and 50. Typical results for the intermittency function are shown in figure 4 for $x/M = 41$. In the lower, cold region of the flow, the distribution follows closely an error

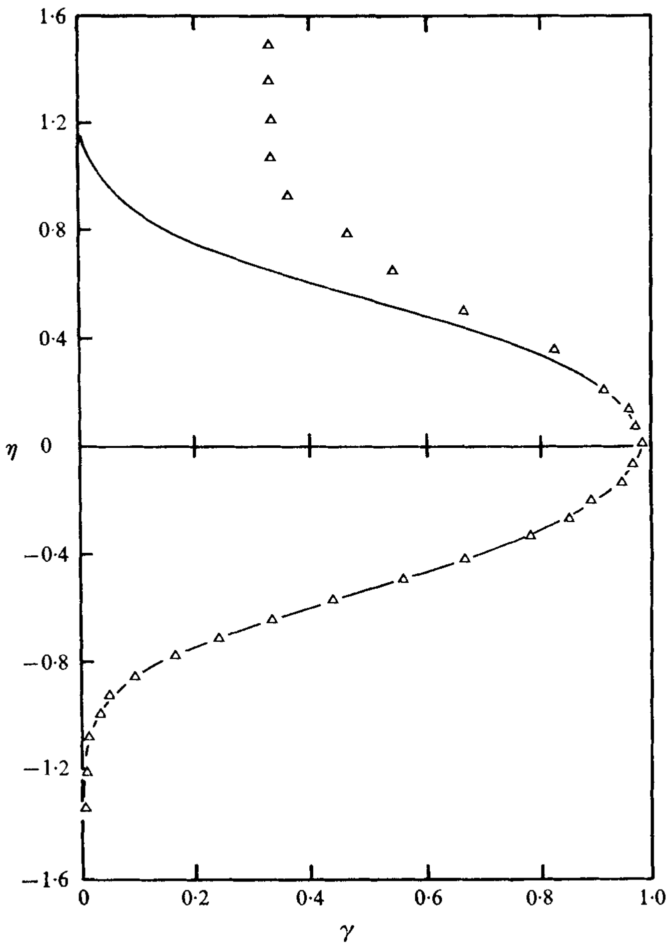

FIGURE 4. Intermittency function; $x/M = 41$.

function. In the upper, warm region, γ asymptotes to a constant of about 0·3. This is a consequence of assuming symmetrical variation of the threshold level for the two zones. In principle, it would have been possible to 'recalibrate' C_1 from these results, forcing γ to approach zero at roughly $\eta = 1$. However, it was decided to leave the data in this form to emphasize the differences in the structure of the hot and cold bursts. The differences can be seen clearly from the representative traces in figure 3 and it is evident that, in detail, the mixing layer is not truly symmetrical.

Conventional and zone mean distributions are shown for $x/M = 41$ in figure 5. These agree essentially with the picture suggested previously and illustrated by the definition sketch in figure 2. The data are compared with the solution with constant eddy viscosity of Watt & Baines (1973). The scatter of points at the extremities reflects statistical limitations in the treatment of the data. As γ approaches zero or unity, the frequency of bursts of tagged fluid decreases and the absolute number becomes too small for a meaningful average.

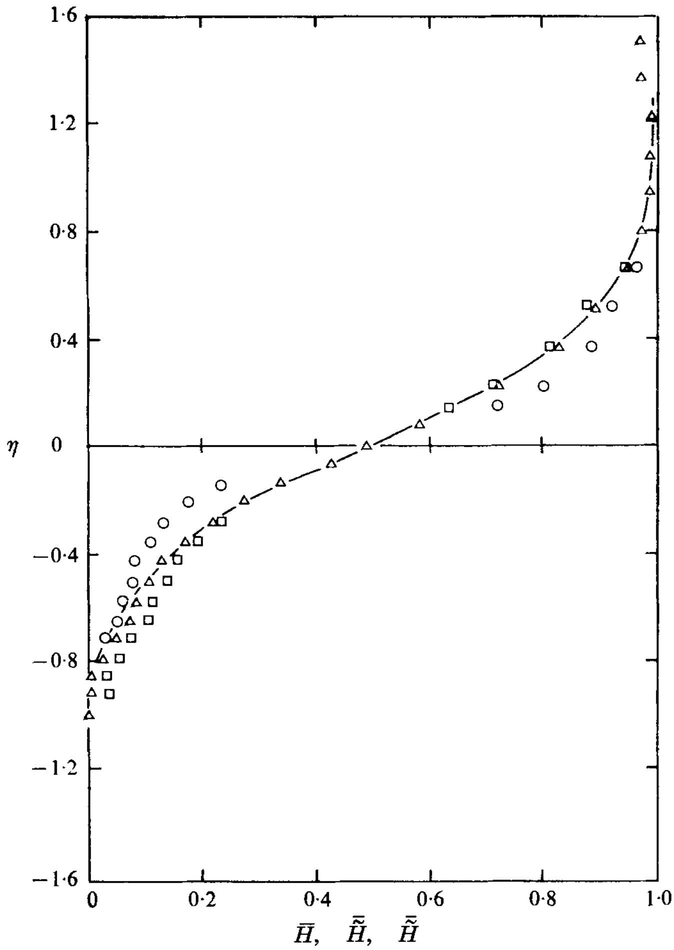

FIGURE 5. Zone-averaged mean temperature; $x/M = 41$. $\triangle$, $\bar{H}$; $\square$, $\tilde{\bar{H}}$; $\bigcirc$, $\bar{\bar{H}}$; ——, $\bar{H} = 0{\cdot}5 + 0{\cdot}5\,\mathrm{erf}\,(\eta/l_\theta)$.

The zone-averaged distributions of fluctuation intensity are shown in figure 6 for the same streamwise station. In the lower region of the mixing layer the results are consistent, showing the warm bursts to have significantly higher intensity than the cold fluid. Again the distinction is not as clear for the upper region. The problem lies in the large background level of intensity fluctuations generated by the heated rods. Production of $(\overline{\theta^2})^{\frac{1}{2}}$ is large in the region immediately downstream of the rods whereas dissipation or smearing proceeds relatively slowly (see figure 8). The result is that only the largest bursts can be identified by any detection scheme. The problem is analogous to attempts to define a turbulent/non-turbulent interface in those situations where the external 'potential' flow possesses a large background turbulent intensity. Because of this difficulty we shall restrict most of the following discussion to the lower region of the mixing layer, where the distinction between the two fluid states can be made more precisely.

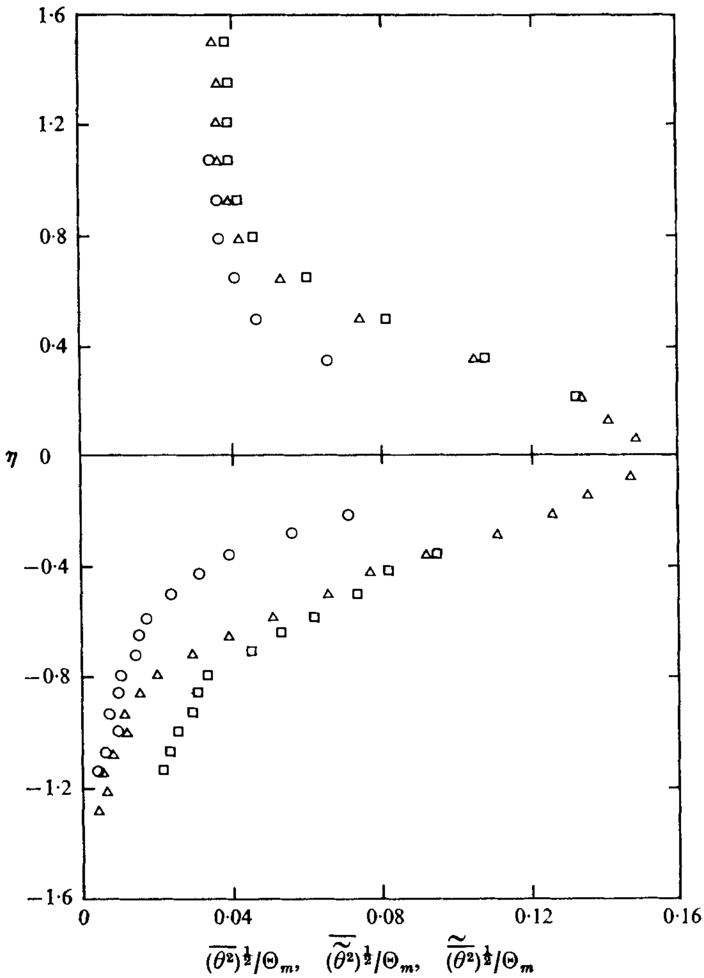

FIGURE 6. Zone-averaged temperature fluctuation intensities; $x/M = 41$. △, $(\overline{\theta^2})^{\frac{1}{2}}/\Theta_m$; □, $(\overline{\tilde{\theta}^2})^{\frac{1}{2}}/\Theta_m$; ○, $(\overline{\tilde{\tilde{\theta}}^2})^{\frac{1}{2}}/\Theta_m$.

Average zone widths were evaluated and are plotted in figure 7 for the representative station $x/M = 41$. The results were made dimensionless using l_θ, which is defined as $y_{\bar{H}=0\cdot9} - y_{\bar{H}=0\cdot1}$ (see figure 1). The curves for the hot and cold zones show the expected trends, decreasing smoothly towards zero as γ approaches zero and unity respectively. The burst rate, normalized by U_0/l_θ, is also plotted in figure 7 and is seen to be a maximum at $\gamma \approx 0\cdot6$. The magnitude of the burst rate is highly sensitive to a number of variables, especially the smoothing time. It is a somewhat arbitrary parameter (Bradshaw & Murlis 1973). Nevertheless the general shape of this function and the position of the maximum are less dependent upon the processing of the signal and are thus an interesting reflexion of the dynamics of the bursting.

The streamwise decay of the thermal fluctuation intensity in the uniformly heated zone is shown in figure 8. The absolute level is high, of the order of 3·7 %

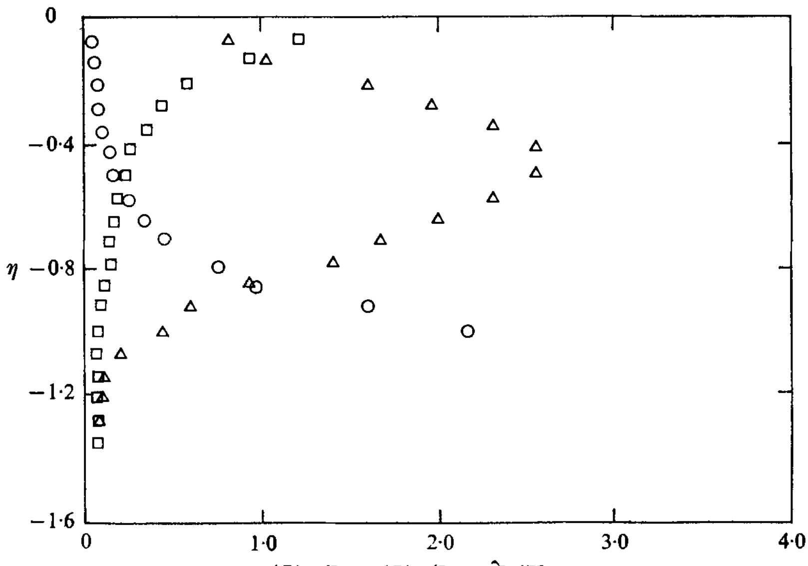

FIGURE 7. Distributions of average zone lengths and burst rate; $x/M = 41$. □, $\langle L\rangle_H/l_\theta$; ○, $\langle L\rangle_C/l_\theta$; △, $\hat{f}l_\theta/U_0$.

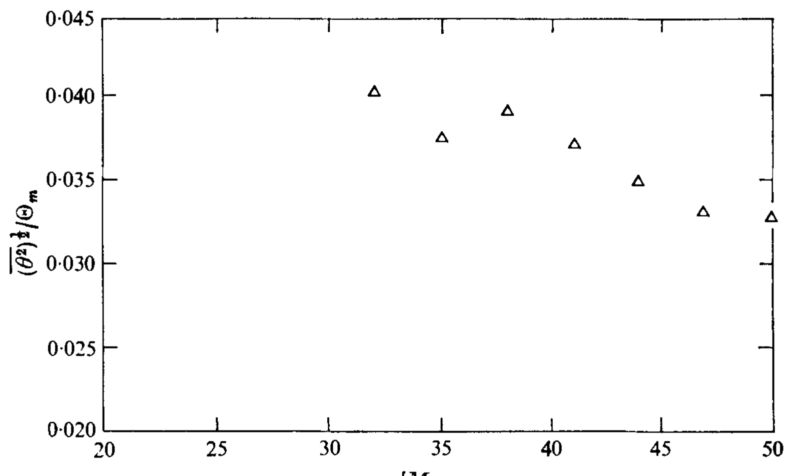

FIGURE 8. Thermal fluctuation intensity in fully hot zone; $\eta = 1{\cdot}32$.

at $x/M = 41$. This is sufficient to exclude small warm pulses from the detection scheme. Furthermore, it is seen that the net dissipation of $\overline{\theta^2}$-stuff is small, the intensity levels changing by less than 1 % over the distance between the first and third streamwise station.

Finally, thermal length scales based on both mean temperature and the half-intermittency point have been evaluated to show the overall spreading characteristics of the flow. These are plotted in figure 9. (l_γ is defined as twice the width $y_{\gamma=1\cdot0}-y_{\gamma=0\cdot5}$.) The magnitudes of the scales are different, as would be

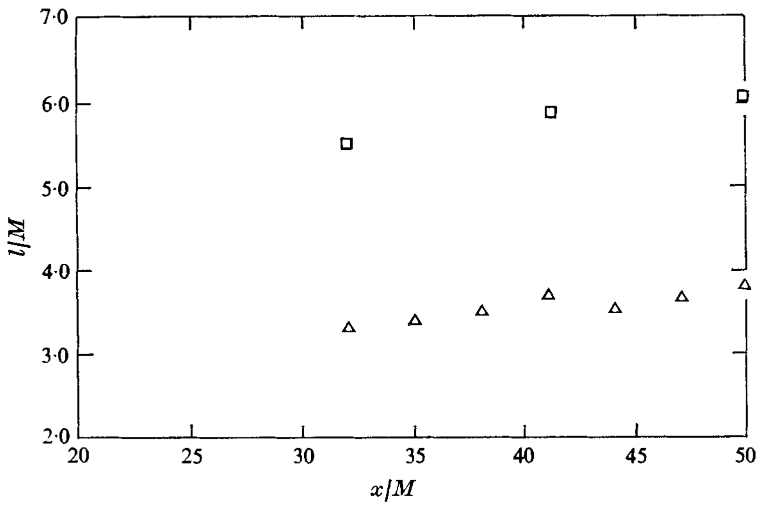

FIGURE 9. Thermal length scales. □, l_{γ}/M; △, l_{θ}/M.

x/M	$(\overline{\theta^2})^{\frac{1}{2}}_{\max}$(°K)
32	0·59
35	0·57
38	0·63
41	0·65
44	0·65
47	0·65
50	0·65

TABLE 3. Variation of thermal fluctuation intensities, $\eta = 0$.

expected, but their variations with downstream distance are identical (as suggested originally by Corrsin & Kistler 1955), each exhibiting a linear lateral growth rate for the thermal mixing layer according to self-preservation theory (Watt 1967).

The variation of the maximum value of the thermal fluctuation intensity is given in table 3. $\partial(\overline{\theta^2})^{\frac{1}{2}}_m/\partial x$ is roughly zero beyond $x/M = 38$, which implies that the flow has reached a state of equilibrium with production and diffusion balancing dissipation. A comparison between the integral scales for the thermal and velocity fields in tables 1 and 2 reveals interesting behaviour. In the fully hot region, L_θ is approximately three times L_u, whereas along the centre-line, where $\gamma = 1{\cdot}0$, they are roughly the same. This reinforces the comment made earlier about the high background level of temperature fluctuations in the zone downstream from the heated rods, where the flow is composed of hot wakes and cold jets.

No attempt has been made to determine the distribution of intensity levels through the hot/cold interface as was done by Hedley & Keffer (1974*a*) for the turbulent/non-turbulent interface for the boundary layer but some general comments can perhaps be made. The transport of heat from the upper to the lower region of the mixing layer will be accomplished by the advective motion of the large turbulent eddies in the flow. The detection scheme is weighted towards these easily identified eddies and the characteristics of the hot/cold interface will be a least partially dependent upon parameters such as the smoothing time and threshold level. Nevertheless, we are able to infer some of the expected properties of the smallest scales. It is unlikely that the sharpness observed by Corrsin & Kistler (1955) and Hedley & Keffer (1974*a*) for the turbulent/non-turbulent interface exists in this present situation. In the former, contamination of the non-turbulent field by vortical fluctuations occurs in the limit, essentially by local intensification of the intensity gradients. In our case, the mechanism of contamination is effected by turbulent diffusion rather than molecular diffusion. The passive contaminant is merely advected by successively smaller scales of the homogeneous turbulent field and it is probable that in the viscous limit dissipation of turbulence and smearing of the scalar proceed together. The problem is fundamentally different from the case of a free shear flow in which the turbulent fluid is marked by a passive scalar. There the interface will be sharply defined by the temperature, say, and vorticity fluctuations and contamination of the non-turbulent fluid will be accomplished by molecular conduction through the superlayer. There is some evidence to suggest that these molecular processes may be different, i.e. that contamination of the non-turbulent fluid by temperature and by vorticity proceed at different rates. Recent results obtained by Davies *et al.* (1975) and Fiedler (1974) indicate heating of the non-turbulent fluid, especially in regions where γ is close to unity. Some further experiments, on a heated two-dimensional wake (Kawall & Keffer 1977), suggest that heating of the 'potential' fluid occurs for $\gamma > 0{\cdot}5$. The attendant low frequency and low amplitude fluctuations may be considered as variations in the mean structure.

This research was sponsored by the National Research Council of Canada through grant A-2746. The authors would like to thank W. D. Baines for his helpful comments on this work.

REFERENCES

Alexopoulos, C. C. & Keffer, J. F. 1971 *Phys. Fluids*, **14**, 216.

Antonia, R. A. & Bilger, R. W. 1974 *Charles Kolling Res. Lab., Sydney, Tech. Note*, F-66.

Bradshaw, P. & Murlis, J. 1973 *Imp. College Aero. Tech. Note*, no. 73–108.

Corrsin, S. 1943 *N.A.C.A. Wartime Rep.* W-94.

Corrsin, S. & Kistler, A. L. 1955 *N.A.C.A. Rep.* no. 1244.

Davies, A. E., Keffer, J. F. & Baines, W. D. 1975 *Phys. Fluids*, **18**, 770.

Fiedler, H. 1974 *Adv. in Geophys.* A **18**, 93.

Gibson, C. H. & Schwarz, W. H. 1963 *J. Fluid Mech.* **16**, 365.

Hedley, T. B. & Keffer, J. F. 1974*a* *J. Fluid Mech.* **64**, 645.

Hedley, T. B. & Keffer, J. F. 1974*b* *J. Fluid Mech.* **64**, 625.

Kawall, J. G. & Keffer, J. F. 1977 To be published.

LaRue, J. C. 1974 *Phys. Fluids*, **17**, 1513.

Mills, R. R. & Corrsin, S. 1959 *N.A.S.A. Memo.* 5-5-59W.

Watt, W. E. 1967 Ph.D. dissertation, University of Toronto.

Watt, W. E. & Baines, W. D. 1973 *J. Hydraul. Res.* **11**, 157.

Wiskind, H. K. 1962 *J. Geophys. Res.* **67**, 3033.